

Glycosylated diazeniumdiolate-based oleanolic acid derivatives: synthesis, *in vitro* and *in vivo* biological evaluation as anti-human hepatocellular carcinoma agents†Zhangjian Huang,^{‡a} Junjie Fu,^{‡a} Ling Liu,^a Yijun Sun,^b Yisheng Lai,^a Hui Ji,^a Edward E. Knaus,^c Jide Tian^d and Yihua Zhang^{*a}

Received 3rd February 2012, Accepted 9th March 2012

DOI: 10.1039/c2ob25252j

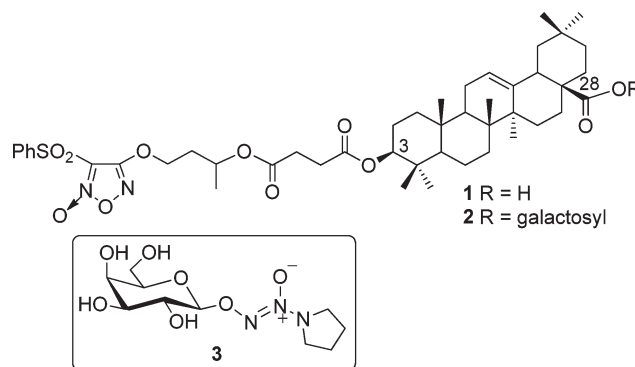
A series of *O*²-glycosylated diazeniumdiolate-based derivatives of oleanolic acid (**4–19**) were synthesized and their anti-human hepatocellular carcinoma (HCC) activities were evaluated. Compound **6** selectively inhibited HCC, but not non-tumor liver cell proliferation. This inhibition was attributed to high levels of nitric oxide (NO) released in HCC cells. Importantly, **6** exhibited low acute toxicity (LD₅₀ = 173.3 mg kg⁻¹) and potent inhibition of HCC tumor growth in mice (3 mg kg⁻¹ iv). Furthermore, **6** induced HCC cell apoptosis, which was accompanied by lower mitochondrial membrane potentials and Bcl2 expression, but with higher cytochrome C release, Bax, caspase 3 and 9 expression activities in HCC cells. Collectively, **6** may be a promising candidate drug for the intervention of HCC.

Introduction

Human hepatocellular carcinoma (HCC) is an aggressive malignancy with a poor prognosis, and is the third leading cause of cancer death worldwide. Development of new therapeutic agents to treat HCC is urgently needed. Currently, there is no effective chemotherapy for HCC.¹ Notably, high levels of NO can induce tumor cell apoptosis^{2,3} and oleanolic acid (OA) possesses a unique property of liver-specific metabolism⁴ and antitumor activity.⁵ Our previous studies have demonstrated that 1,2,5-oxadiazole-2-oxide (furoxan)-based NO releasing derivatives of OA (representative compounds **1** and **2**, Scheme 1) show strong cytotoxicity against HCC *in vitro* and significantly inhibit the growth of HCC tumors *in vivo*.^{6,7} However, these derivatives have a low selective cytotoxicity against HCC, which may cause adverse effects.

Diazeniumdiolate is an attractive alternative type of nitric oxide (NO) donor that is able to release high levels of NO (two

molecules of NO from per molecule of diazeniumdiolate) under physiological conditions.⁸ Given the benefit of releasing a larger amount of NO, the utility of diazeniumdiolates has been examined in various aspects of antitumor therapy.^{9,10} Importantly, the precise *O*²-protection of diazeniumdiolates may limit the release of high levels of NO in non-tumor tissue or cells, thereby minimizing unwanted adverse effects. For example, the *O*²-glycosylated diazeniumdiolate **3** (Scheme 1) requires glycosidase cleavage to selectively furnish the diazeniumdiolate that then releases NO to provide significant antitumor activity.^{11,12} Furthermore, glycosyl derivatives of a NO donor can be recognized by glucose transporter proteins and asialoglycoprotein receptors (ASGPR), which are highly expressed in human HCC cells, thus



Scheme 1 Chemical structures of furoxan-based OA derivatives **1** and **2** with potent anti-HCC activities, and one representative *O*²-glycosylated diazeniumdiolate **3**.

^aCenter of Drug Discovery, China Pharmaceutical University, Nanjing, P.R. China. E-mail: zyhtgd@163.com; Fax: +86-25-83271015; Tel: +86-25-83271015

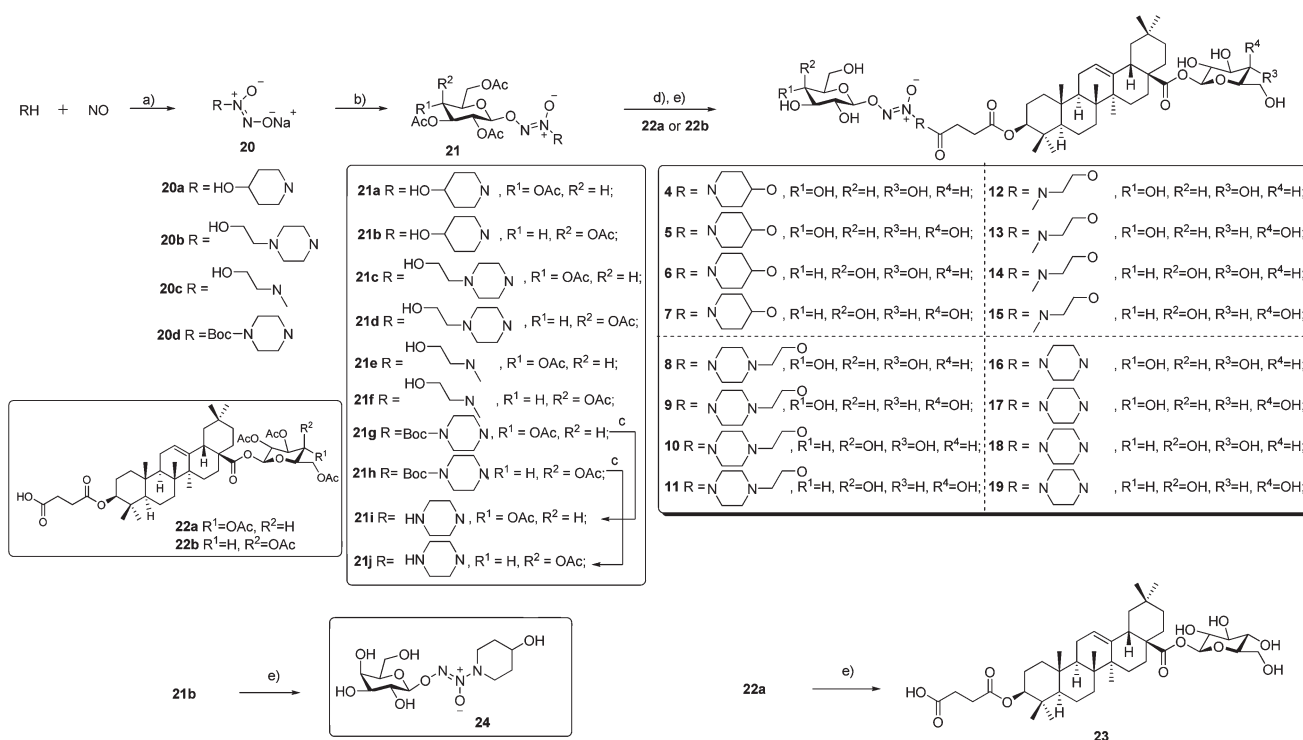
^bNanjing Keygen Biotech. Co., Nanjing, P.R. China

^cFaculty of Pharmacy and Pharmaceutical Sciences, University of Alberta, Edmonton, Alberta T6G 2N8, Canada

^dDepartment of Molecular and Medical Pharmacology, University of California-Los Angeles, Los Angeles, California 90095, USA

†Electronic supplementary information (ESI) available: The preparative procedures and spectrum data for *O*²-glycosylated diazeniumdiolates **21a–j** and **24**, HPLC conditions, chromatograms of **21a–j**, **4–19** and **24**. See DOI: 10.1039/c2ob25252j

‡These authors contributed equally to this work.



Scheme 2 The synthetic route used to prepare compounds **4–19**, **23** and **24**. Reactions and conditions: (a) NaOMe–MeOH–Et₂O, nanometer-sized TiO₂, 25 °C, 48 h. (b) 2,3,4,6-tetra-*O*-acetyl- α -D-glucopyranosyl bromide or 2,3,4,6-tetra-*O*-acetyl- α -D-galactopyranosyl bromide, DMF, K₂CO₃, –20 °C, 12 h. (c) CF₃COOH, CH₂Cl₂, 3–4 h. (d) DCC, DMAP, anhydrous CH₂Cl₂, 25 °C, 24 h. (e) NaOMe–MeOH–CH₂Cl₂, 0–10 °C, 30 min.

enhancing glycosylated NO donor's selectivity and cytotoxicity.^{13,14} Accordingly, we hypothesized that *O*²-glycosylated diazeniumdiolate derivatives of OA would exhibit potent cytotoxicity selectively against HCC. Herein, we describe the synthesis of a group of *O*²-glycosylated diazeniumdiolate derivatives of OA **4–19**, their ability to release NO, *in vitro* and *in vivo* anti-HCC activities, and possible mechanisms underlying their actions.

Results

Chemistry

The synthetic route used to prepare **4–19** is depicted in Scheme 2. Three secondary amines possessing a free hydroxyl group (4-hydroxypiperidine, *N*-(2-hydroxyethyl)piperazine or *N*-methylethanolamine) and 1-Boc-piperazine were allowed to react with NO gas at atmospheric pressure in the presence of a catalytic amount of nanometer-sized TiO₂ at room temperature. These respective reactions furnished the corresponding diazeniumdiolate sodium salts **20a–d**, according to our previous protocol.¹⁵ *O*²-Glycosylation of **20a–d** with 2,3,4,6-tetra-*O*-acetyl- α -D-glucopyranosyl bromide, or 2,3,4,6-tetra-*O*-acetyl- α -D-galactopyranosyl bromide, resulted in the respective *O*²-glycosylated diazeniumdiolates **21a–h**. Deprotection of **21g** and **21h** with trifluoroacetic acid afforded amino compounds **21i** and **21j**. Coupling of eight diazeniumdiolate compounds **21a–f**, **21i** or **22j** with the OA compounds **22a** or **22b**,⁷ respectively, in the presence of dicyclohexylcarbodiimide (DCC) and 4-*N*,*N*-dimethylaminopyridine (DMAP), followed by direct deacetylation

using NaOMe in anhydrous MeOH and CH₂Cl₂ and subsequent neutralization with acidic ion exchange resin, provided sixteen target compounds **4–19**. Similar deacetylation of **22a** and **21b** produced compounds **23** and **24**, respectively (Scheme 2).

In vitro biological assessment

Anti-HCC activity was determined by incubating human HCC SMMC-7721 cells with different concentrations of each test compound for 48 h. The inhibitory effects of individual compounds **4–19** on the proliferation of human HCC SMMC-7721 cells were measured by MTT assay¹⁶ using 5-fluorouracil (5-FU), **1** and **2** as positive controls. Their IC₅₀ values (a dose that achieved 50% inhibition of cancer cell proliferation) are presented in Fig. 1a (data for **18** and **19** with a IC₅₀ of >100 μ M are not shown). The potency of **4–6** (IC₅₀ = 3.45–4.21 μ M range) were of the same order of magnitude as for **1** and **2**, but significantly more potent than that of 5-FU (45.1 μ M). Interestingly, **6** displayed more potent inhibition (IC₅₀ = 3.13 μ M) against the proliferation of human HepG2 cells than that of **1** and **2** (IC₅₀ = 15.37 and 5.71 μ M, respectively, Fig. 1b).

Next, it was found that compound **6** (2–8 μ M) inhibited HepG2 cell proliferation in a concentration-dependent manner, but **6** had little inhibitory effect on non-tumor liver LO2 cell proliferation *in vitro*, that is indicative of a selective cytotoxicity against HCC cells (Fig. 2a). Furthermore, it was found that incubation with **6** (10 μ M), or the diazeniumdiolate glycoside **24**, but not the OA compound **23** lacking the NO donor moiety, inhibited the proliferation of HepG2 cells in a time-dependent manner

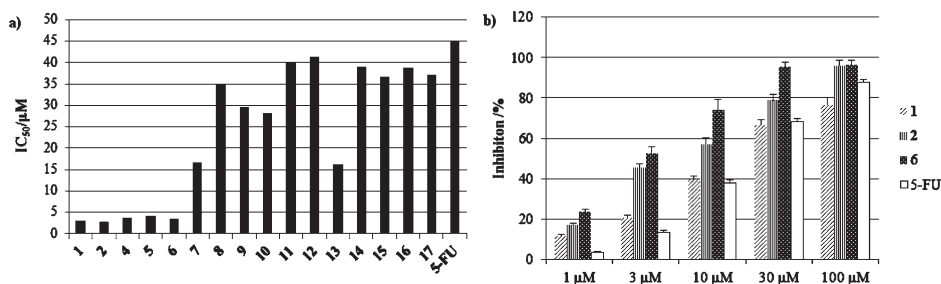


Fig. 1 Inhibitory activities of target compounds against HCC cells. (a) IC_{50} values for compounds **1**, **2**, **4**–**17** and 5-FU in SMMC-7721 cells. (b) Inhibitory activities of compounds **1**, **2**, **6** and 5-FU against HepG2 cells. Data are expressed as mean or mean \pm SEM value of each compound from three separate measurements.

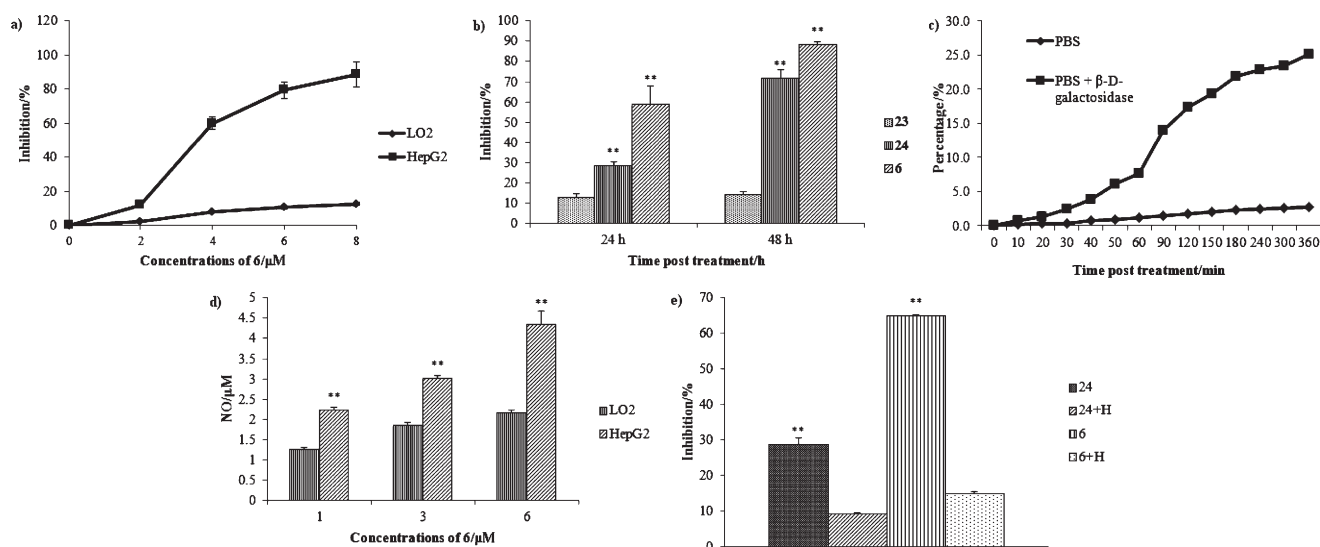


Fig. 2 *In vitro* biological assessments of **6**, **23** and **24**. (a) Inhibitory effect of **6** on the proliferation of HepG2 and LO2 cells. HepG2 and LO2 cells were incubated in triplicate with, or without, the indicated concentrations of **6** for 48 h. Cell proliferation was determined using a MTT assay. (b) Inhibitory activity of **6**, **23** and **24** against HepG2 cells. HepG2 cells were incubated in triplicate with, or without, 10 μ M of **6**, **23** and **24** for 24 or 48 h, and the cell proliferation was determined by MTT assay. Data are means \pm SEM of the inhibition (%) for three independent experiments. (c) Quantitative measurement of NO production. Compound **6** (50 μ M) was cultured in triplicate in vehicle PBS (■, pH 7.4) or PBS containing β -D-galactosidase (◆, 10 μ g mL⁻¹) at 37 °C for 6 h and the levels of NO released were determined using a calorimetric Griess reaction assay. Percentage NO release was based on a theoretical maximum release of 2 mol of NO from 1 mol of **6**. Data are the mean value of NO released from three independent measurements ($n = 3$) and intra-group variation from the mean % value was $\leq 0.2\%$. (d) The levels of nitrite/nitrate. HepG2 and LO2 cells were incubated in triplicate with the indicated concentrations of **6** for 6 h and the levels of intracellular nitrite/nitrate were determined using a calorimetric Griess reaction assay. Data are expressed as mean \pm SEM of individual groups of cells from three separate experiments. (e) Effect of haemoglobin (H) on the activity of **6** and **24**. HepG2 cells were pretreated with, or without, 10 μ M haemoglobin for 1 h and then exposed to 10 μ M **6** or **24** for 48 h, respectively. Cell proliferation was determined by MTT assays. Data are expressed as mean \pm SEM of individual groups of cells from three separate experiments. ** $P < 0.01$ vs. **23** (2b), LO2 (2d), or haemoglobin treated (2e), respectively.

(Fig. 2b). Notably, the inhibitory effect of **6** was significantly more potent than that of **23**, and moderately more potent than that of **24**. These data suggest that (i) NO release from the diazeniumdiolate is crucial for its anti-HCC effect, and (ii) the synergistic effects of NO release in conjunction with the inhibitory activity shown by OA are responsible for the high inhibitory effect of **6** upon HCC cell proliferation. Indeed, treatment of **6** with β -D-galactosidase (pH 7.4, 37 °C, 6 h) significantly increased the release of NO as expected, relative to that observed for the vehicle PBS control (Fig. 2c). Apparently, **6** is a relatively stable compound from which NO release is enhanced by the enzyme catalyst galactosidase. Credence for this observation is

consistent with the fact that treatment with **6** resulted in higher levels of NO release in HepG2 cells relative to that in LO2 cells (Fig. 2d). More importantly, treatment with 10 μ M haemoglobin, a known NO quencher,¹⁷ abolished or significantly reduced the anti-HCC activity of **6** and **24** (Fig. 2e), further demonstrating the importance of NO release in the anti-HCC activity of **6**. Collectively, our data indicate that **6** releases high levels of NO and that **6** has potent and selective cytotoxicity against HCC cells. This highly selective cytotoxicity may be attributed to the fact that **6** is able to effectively enter tumor cells due to its interaction with glucose transporter proteins and/or ASGPR, which are highly expressed on human HCC cells, and that high levels of

Table 1 Acute toxicity of **6** in mice

Dose mg kg ⁻¹	Number of mice	Mouse mortality				Total mortality	Survival (%) on day 14
		1 h	4 h	2 d	3–14 d		
200	10	0	8	0	0	8	20
180	10	0	6	0	0	6	40
162	10	0	4	1	0	5	50
145.8	10	0	0	0	0	0	100

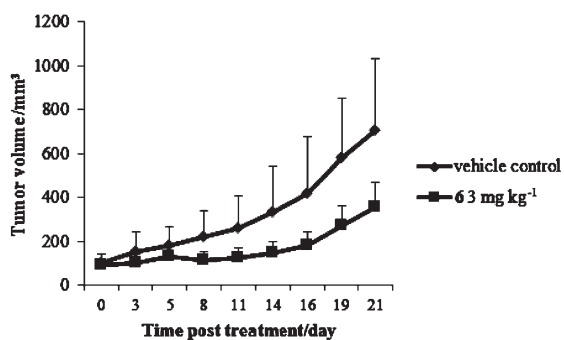


Fig. 3 Effect of **6** on the growth of HCC tumors *in vivo*. Groups of BALB/c nude mice were inoculated with SMMC-7721 cells. When mice displayed a small solid tumor, the mice were randomly treated with either **6**, or vehicle, three times per week and the growth of tumors were measured at the indicated time points. Data shown are mean \pm SEM of tumor volumes from each group of mice ($n = 12$ for vehicle control group and $n = 6$ for the group treated with **6**). * $P < 0.05$ relative to the vehicle control.

NO are released following glycosidic bond cleavage by galactosidase in HCC cells.

In vivo anti-HCC activity of **6**

It is plausible that the *O*²-glycosylated diazeniumdiolate **6** will have a good safety profile due to the selective release of high levels of NO in HCC cells. Accordingly, groups of mice were injected intravenously with a single dose of **6** at 200, 180, 162 and 145.8 mg kg⁻¹ respectively, to assess its acute toxicity. Survival of mice was monitored up to 14 days after injection. Only two mice that had been treated with **6** at the highest dose (200 mg kg⁻¹) survived (Table 1). In contrast, injection with **6** at the lowest dose (145.8 mg kg⁻¹) did not cause any death and abnormality in eating, drinking, body weight, and activity throughout the observation period. As a result, **6** showed a LD₅₀ of 173.3 mg kg⁻¹ that was much larger than that for **2** (LD₅₀ = 91.4 mg kg⁻¹),⁷ suggesting that diazeniumdiolate moiety in **6** may have a safe profile superior to its peer furoxan in this strain of mice using the same assay.

BALB/c nude mice were inoculated subcutaneously with SMMC-7721 cells to evaluate the *in vivo* anti-HCC activity of **6**. When the mouse tumor had grown to 5–7 mm in one dimension, the mice were randomly administered a 3 mg kg⁻¹ intravenous dose of **6**, or vehicle as control, three times per week for three weeks, and tumor growth was monitored by measurement of tumor volume every three days (Fig. 3). This study showed that

Table 2 Treatment with **6** inhibits the growth of tumors *in vivo*^a

Treatment	Dose (mg kg ⁻¹)	Tumor volume (mm ³)	Tumor weight (g)
Vehicle	10	707.2 \pm 322.6	0.72 \pm 0.22
6	3	353.9 \pm 115.6 ^b	0.27 \pm 0.09 ^c

^aData shown are the mean \pm SD of tumor volumes and weights for each group of mice ($n = 12$ for the vehicle control group and $n = 6$ for the group treated with **6**). ^b $P < 0.05$ relative to the vehicle control group, determined by the Mann–Whitney U test. ^c $P < 0.01$ relative to the vehicle control group, determined by the Mann–Whitney U test.

treatment with **6** (3 mg kg⁻¹ iv dose 3 times per week for 3 weeks) significantly reduced the volumes of HCC tumors. In this regard, the mean tumor size (volume) and weight in mice treated with **6** were significantly lower than the tumors in vehicle-treated control mice (Table 2).

It is relevant that there was no statistical difference in the average percentage change in body weights post inoculation between these two groups of mice (data not shown). Together, these results demonstrate that the *O*²-glycosylated diazeniumdiolate-based OA compound **6** is a potent inhibitor of HCC tumors in mice, and that it has a lower toxicity than the furoxan-based galactosyl ester **2**.⁷

Possible mechanisms underlying the anti-HCC activity exhibited by compound **6**

To determine the effect of **6** on HCC cell apoptosis, SMMC-7721 cells were incubated with different concentrations of **6**, or OA, for 48 h, and the percentages of apoptotic HCC cells were determined by FITC-Annexin V/PI staining and flow cytometry. As shown in Fig. 4, the percentage of annexin V + apoptotic HCC cells gradually increased for those cells exposed to increasing concentrations of **6**, demonstrating that incubation with **6** induced HCC cell apoptosis in a concentration-dependent manner. In contrast, incubations performed using the same concentrations of OA did not promote HCC cell apoptosis (data not shown).

High levels of NO can induce oxidative stress, which can induce cell apoptosis through caspase-dependent and independent pathways, particularly by the intrinsic mitochondrial pathway.^{18,19} During the process of apoptosis, apoptotic signals can result in the loss of mitochondrial membrane potential ($\Delta\Psi_M$), the release of cytochrome C from mitochondria to cytoplasm, a down-regulation of anti-apoptotic protein Bcl2, and an up-regulation of pro-apoptotic protein Bax, leading to activation of caspases 3 and 9.^{20–24} To determine plausible pathways by which **6** triggered HCC cell apoptosis, SMMC-7721 cells were incubated with different concentrations (0, 1.5, 3.0, 6.0 μ M) of **6** for 48 h prior to staining with the lipophilic mitochondrial probe 5,5',6,6'-tetrachloro-1,1',3,3'-tetraethylbenzimidazol-carbocyanine iodide (JC-1). The number of HCC cells with collapsed mitochondrial membrane potentials in different groups of cells were determined by flow cytometry analysis (Fig. 5). These studies showed that incubation with **6** increased the number of HCC cells with collapsed mitochondrial membrane potentials.

Further Western blotting analysis revealed that incubation with **6** dramatically increased the relative levels of pro-apoptotic cytochrome C, Bax, caspase 3 and caspase 9 expression, but reduced the levels of anti-apoptotic Bcl2 expression (Fig. 6a and b) in a concentration-dependent manner. Subsequent experiments to examine the levels of activated caspase 3 and 9 using enzymatic calorimetric assays kits showed that incubation with **6** elevated the levels of activated caspase 3 and 9 activities in a concentration-dependent manner (Fig. 6c). The increased number of HCC cells with collapsed mitochondrial membrane potentials,

and an elevated level of caspase 3 and 9 expression, suggest that **6** induces HCC apoptosis through oxidative stress-triggered mitochondria-related caspase 3 and 9-dependent pathways. We are currently interested in further studies to investigate how NO-releasing compounds promote HCC cell apoptosis.

Discussion and conclusions

Structure–activity relationship (SAR) analysis revealed that the target compounds **16–19** with an amide bond connecting the OA moiety to the diazeniumdiolate showed much less cytotoxicity compared to compounds **4–15** with an ester linker. It is possible that these ester compounds may be more easily metabolized to release NO than the amide compounds. The secondary amine moiety connected to the *N*¹-atom of the diazeniumdiolate moiety in **4–15** may be a determinant of anti-HCC activity given that the relative potency order was 4-hydroxypiperidine > *N*-(2-hydroxyethyl)piperazine > *N*-methylethanolamine. Furthermore, there was no significant difference in anti-HCC activity between the *O*²-glucosyldiazeniumdiolate compounds and *O*²-galactosyldiazeniumdiolate compounds (**4, 5** vs. **6, 7, 8, 9** vs. **10, 11, 12, 13** vs. **14, 15** and **16, 17** vs. **18, 19**, respectively). In this regard, it is possible that these glucosyl and galactosyl modified derivatives may interact with both glucose transporter proteins and asialoglycoprotein receptors (ASGPR) that are highly expressed on human HCC cells, allowing these glycoside derivatives to enter into the cells by endocytosis.^{13,14} Support for this belief is in agreement with the observation that **6** exhibits a potent and selective cytotoxicity against HCC cells that may be attributed to its efficient entry into the cells and the high levels of NO selectively released in HCC cells. More importantly, the *O*²-glycosylated diazeniumdiolate-based OA compound **6** possesses a low acute toxicity and administration of **6** at a low dose (3 mg kg⁻¹ iv) significantly inhibited the growth of HCC tumors in mice relative to that observed for the less potent furoxan-based OA derivative **2**.⁷ One plausible explanation for this observation is that the diazeniumdiolate moiety in **6** can selectively release more NO in tumor cells relative to furoxan-based OA derivative **2**. Furthermore, it was found that incubation with **6** induced apoptosis in HCC cells, mitochondrial membrane potentials and anti-apoptotic Bcl2 expression were lowered. In contrast, increased cytochrome C release and pro-apoptotic Bax,

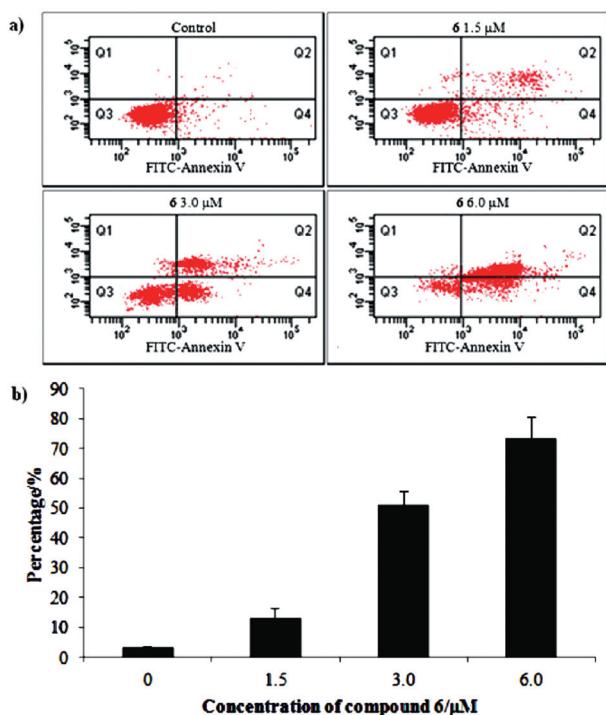


Fig. 4 Compound **6** induces SMMC-7721 cell apoptosis *in vitro*. SMMC-7721 cells were incubated with the indicated concentrations of **6** or OA for 48 h and the cells were stained with FITC-Annexin V and PI, followed by flow cytometry analysis. (a) Flow cytometry analysis. (b) Quantitative analysis of apoptotic cells. Data are representative flow cytometry charts that are illustrated as mean \pm SEM of the percentages of apoptotic cells from three independent experiments.

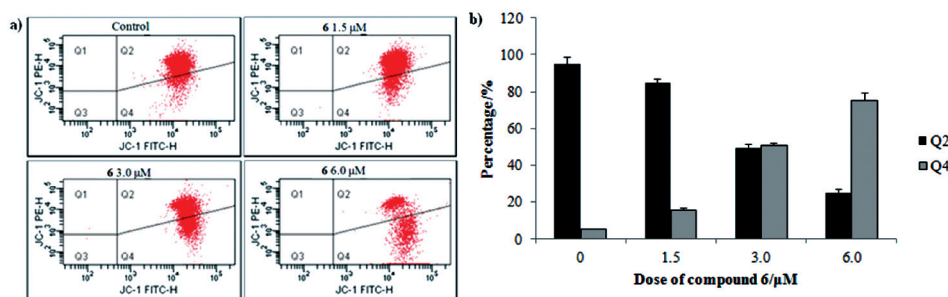


Fig. 5 Effect of **6** on the mitochondrial membrane potentials of SMMC-7721 cells. SMMC-7721 cells were incubated with the indicated concentrations of **6** for 48 h prior to staining with JC-1. The percentage of cells with healthy or collapsed mitochondrial membrane potentials was determined by flow cytometry analysis. Data for representative charts are illustrated as mean \pm SEM for the percentages of cells in different phases from three separate experiments.

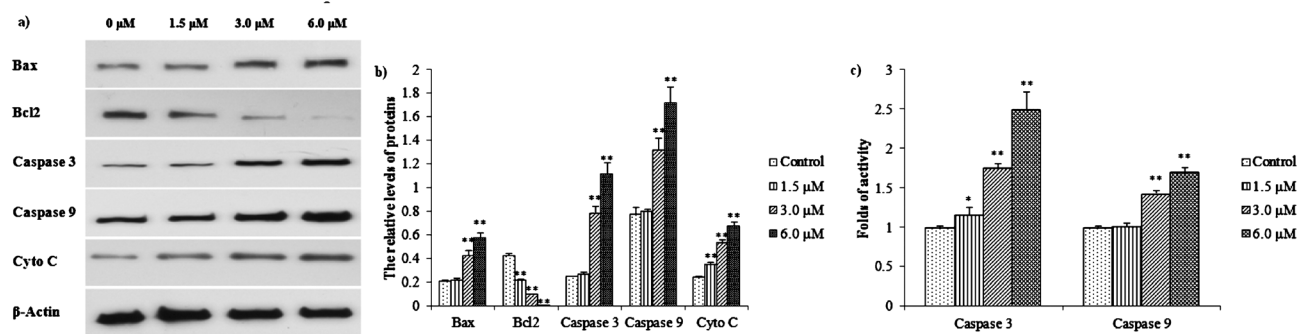


Fig. 6 Effect of **6** on the expression of apoptosis-related proteins in SMMC-7721 cells. (a) The expression of Bax, Bcl2, caspase 3 and 9, cyto-C, and β -actin was examined by Western blot analysis. SMMC-7721 cells were incubated with, or without, **6** at the indicated concentrations for 48 h and the levels of protein expression were detected using specific antibodies. Data shown are representative images of each protein for three separate experiments. (b) Quantitative analysis: the relative levels of each protein compared to control β -actin were determined by densitometric scanning. Data are expressed as means \pm SEM from three separate experiments. (c) The activities of caspase 3 and 9: SMMC-7721 cells were incubated with, or without, **6** at the indicated concentrations for 48 h and the cells were harvested. The contents of activated caspase 3 or 9 in the cell lysates was analyzed using a colorimetric assay. Data are expressed as means \pm SEM for the relative activities of each group of cells from three separate experiments where the activity of control cells without **6** treatment was designated as 1. * $P < 0.05$ vs. the vehicle control. ** $P < 0.01$ vs. the vehicle control.

caspase 3 and 9 expression was observed in HCC cells. Apparently, **6** induces HCC cell apoptosis *via* oxidative stress-triggered mitochondria-related caspase-dependent pathways. The selective *in vitro* anti-HCC activity, low acute toxicity and high inhibition of HCC tumor growth in mice treated with **6** make it a promising candidate drug for the intervention of HCC. It is expected that the mechanistic and biological studies described in this investigation will facilitate the design of new therapeutic agents for the clinical intervention of HCC disease.

Experimental section

General

Melting points were determined on a Mel-TEMP II melting point apparatus which was uncorrected. Infrared (IR) spectra (KBr) were recorded using a Nicolet Impact 410 instrument (KBr pellet). ^1H NMR spectra were recorded with a Bruker Avance 300 MHz spectrometer at 300 °K, using TMS as an internal standard. MS spectra were recorded on a Shimadzu GC-MS 2010 (EI) or a Mariner Mass Spectrum (ESI). Analytical and preparative TLC were performed on silica gel (200–300 mesh) GF/UV 254 plates and the chromatograms were visualized under UV light at 254 and 365 nm. All solvents were reagent grade and, when necessary, were purified and dried by standards methods. The purity of all compounds tested was characterized by the HPLC analysis (LC-10A HPLC system consisting of LC-10ATvp pumps and SPD-10Avp UV detector) and high resolution mass spectrometry (Agilent technologies LC/MSD TOF). Individual compounds with a purity of $>95\%$ were used for subsequent experiments (see the ESI†).

2,3,4,6-Tetra-*O*-acetyl- α -D-glucopyranosyl bromide, 2,3,4,6-tetra-*O*-acetyl- α -D-galactopyranosyl bromide, **22a**, **22b** and **23** were synthesized, as previously described.¹¹ Sodium diazeniumdiolates **20a–d** were prepared according to the method described previously.¹⁵ All animal experiments were performed in accordance with the Animals (Scientific Procedures) Act 2009

(P R China), and all animal experimental protocols were approved and guided by the Animal Research Protection Committee of China Pharmaceutical University, Nanjing, China.

General procedure for the preparation of compounds 4–19

A mixture of an *O*²-glycosylated diazeniumdiolate (1 mmol), 3-oxy-monosuccinate-oleanolic acid-28- β -D-(2,3,4,6-tetra-*O*-acetyl)-glycosyl ester (1 mmol), DCC (309 mg, 1.5 mmol) and DMAP (183 mg, 1.5 mmol) in anhydrous CH_2Cl_2 (10 mL) was stirred at room temperature for 12 h at which time the TLC indicated that the starting materials were totally consumed. After filtration, the filtrate was concentrated and the residue was dissolved in the 1 : 1 mixture of anhydrous CH_2Cl_2 and MeOH at ice-bath temperature and MeONa in methanol solution (30%, 0.923 mL) was added drop wise. The deacetylation procedure was monitored by TLC and upon completion the reaction mixture was neutralized with acidic ion exchange resin 001 \times 7 (732). After filtration, the filtrate was evaporated in vacuo and the resulting residue was purified by column chromatography (MeOH- CH_2Cl_2 1 : 10 v/v) to furnish the respective title product.

***O*²- β -D-Glucopyranosyl-1-{4-[(12-en-28- β -D-glucopyranosyl-oleanolate-3-yl-oxy)-succinyl-oxy] piperidin-1-yl}diazen-1-ium-1,2-diolate (4).** The title product was obtained in 33% yield as a white powder; mp 103–105 °C; IR (KBr, cm^{-1}): 3425, 2946, 1733, 1641, 1462, 1257, 1164, 1073, 1010; ^1H NMR (DMSO- d_6 , 300 MHz): δ 0.69 (s, 3H, CH_3), 0.80 (s, 3H, CH_3), 0.88 (s, 6H, 2 \times CH_3), 1.02–1.04 (m, 3H, CH_3), 1.09 (s, 3H, CH_3), 4.01–4.06 (m, 1H, H_3), 4.34–4.35 (m, 1H, H_3), 4.41–4.42 (m, 2H, 2 \times H_5), 4.58–4.64 (m, 1H, 3 α -H), 4.79–4.87 (m, 1H, OCH), 4.89–4.91 (m, 1H, H_4), 4.94–4.96 (m, 1H, H_2), 5.02–5.04 (m, 2H, H_6' and H_2), 5.12–5.14 (m, 1H, H_6'), 5.16–5.18 (m, 2H, 2 \times H_6), 5.22–5.25 (m, 1H, H_1), 5.41–5.43 (m, 1H, H_1). ESI-MS: 1022 [M - H]⁻; 1058 [M + Cl]⁻; 1041 [M + NH_4]⁺; HRMS: calculated for $\text{C}_{51}\text{H}_{81}\text{N}_3\text{O}_{18}\text{Na}$ [M + Na]⁺: 1046.5407, found: 1046.5405, PPM error -0.19.

***O*²-β-D-Glucopyranosyl 1-{4-[(12-en-28-β-D-galactopyranosyl-oleanolate-3-yl-oxy)-succinyl-oxy] piperidin-1-yl} diazen-1-ium-1,2-diolate (5).** The title product was obtained in 28% yield as a white powder; mp 107–109 °C; IR (KBr, cm⁻¹): 3435, 2948, 1736, 1643, 1459, 1230, 1165, 1075; ¹H NMR (DMSO-d₆, 300 MHz): δ 0.69 (s, 3H, CH₃), 0.80 (s, 6H, 2 × CH₃), 0.88 (s, 6H, 2 × CH₃), 1.10 (s, 3H, CH₃), 1.24 (s, 3H, CH₃), 2.57 (s, 4H, 2 × COCH₂), 2.73–2.77 (m, 1H, C₁₈-H), 3.17–3.23 (m, 4H, 2 × NCH₂), 3.39–3.42 (m, 4H, 2 × OCH₂), 3.47–3.50 (m, 2H, 2 × H₃), 3.65–3.70 (m, 2H, 2 × H₅), 4.38–4.41 (m, 2H, 2 × H₄), 4.49–4.51 (m, 1H, H₂), 4.55–4.60 (m, 1H, 3α-H), 4.74–4.77 (m, 1H, H₂), 4.80–4.87 (m, 1H, OCH), 4.89–4.96 (m, 1H, H₆), 4.98 (d, *J* = 6.0 Hz, 1H, H₆), 5.03 (d, *J* = 5.4 Hz, 1H, H₆), 5.13–5.16 (m, 2H, H₆ and C₁₂-H), 5.21 (d, *J* = 7.8 Hz, 1H, H₁), 5.40–5.42 (m, 1H, H₁); ESI-MS: 1022 [M – H]⁻; 1058 [M + Cl]⁻; HRMS: calculated for C₅₁H₈₁N₃O₁₈Na [M + Na]⁺: 1046.5407, found: 1046.5388, PPM error –1.82.

***O*²-β-D-Galactopyranosyl 1-{4-[(12-en-28-β-D-glucopyranosyl-oleanolate-3-yl-oxy)-succinyl-oxy] piperidin-1-yl} diazen-1-ium-1,2-diolate (6).** The title compound was obtained in 29% yield as a white powder; mp 106–108 °C; IR (KBr, cm⁻¹): 3421, 2946, 1734, 1654, 1457, 1162, 1074; ¹H NMR (CDCl₃, 300 MHz): δ 0.69 (s, 3H, CH₃), 0.80 (s, 6H, 2 × CH₃), 0.88 (s, 9H, 3 × CH₃), 1.09 (s, 3H, CH₃), 2.57 (s, 4H, 2 × COCH₂), 3.38–3.52 (m, 6H, 2 × H₅ and 2 × NCH₂), 3.60–3.63 (m, 1H, H₃), 3.67 (s, 1H, H₃), 4.39–4.42 (m, 2H, H₄ and 3α-H), 4.51 (d, 1H, *J* = 3.5 Hz, H₄), 4.63 (brs, 1H, H₂), 4.82–4.87 (m, 3H, OCH and 2 × H₆), 4.93 (s, 1H, H₂), 4.99 (brs, 1H, C₁₂-H), 5.13 (d, *J* = 5.0 Hz, 1H, H₆), 5.17 (brs, 1H, H₆), 5.22–5.25 (m, 2H, 2 × H₁); ESI-MS: 1041 [M + NH₄]⁺; HRMS: calculated for C₅₁H₈₁N₃O₁₈Na [M + Na]⁺: 1046.5407, found: 1046.5416, PPM error 0.86.

***O*²-β-D-Galactopyranosyl 1-{4-[(12-en-28-β-D-galactopyranosyl-oleanolate-3-yl-oxy)-succinyl-oxy]piperidin-1-yl} diazen-1-ium-1,2-diolate (7).** The title compound was obtained in 25% yield as a white powder; mp 104–106 °C; IR (KBr, cm⁻¹): 3421, 2947, 1732, 1642, 1468, 1162, 1147, 1072. ¹H NMR (CDCl₃, 300 MHz): δ 0.69 (s, 3H, CH₃), 0.80 (s, 6H, 2 × CH₃), 0.87–0.88 (m, 9H, 3 × CH₃), 1.09 (s, 3H, CH₃), 2.56 (s, 4H, 2 × COCH₂), 2.73–2.76 (m, 1H, C₁₈-H), 3.66–3.68 (m, 2H, 2 × H₃), 4.38–4.41 (m, 1H, H₄), 4.47 (d, *J* = 4.2 Hz, 1H, H₂), 4.49–4.53 (m, 2H, H₂ and H₄), 4.62 (t, *J* = 5.3 Hz, 1H, 3α-H), 4.73 (d, *J* = 5.3 Hz, 1H, H₆), 4.82–4.86 (m, 3H, H₆, H₆ and OCH), 4.94 (d, *J* = 5.7 Hz, 1H, H₆), 5.16 (brs, 1H, C₁₂-H), 5.20–5.22 (m, 2H, 2 × H₁); ESI-MS: 1022 [M – H]⁻, 1058 [M + Cl]⁻; 1041 [M + NH₄]⁺; HRMS: calculated for C₅₁H₈₁N₃O₁₈Na [M + Na]⁺: 1046.5407, found: 1046.5399, PPM error –0.76.

***O*²-β-D-Glucopyranosyl 1-{*N*-[(12-en-28-β-D-glucopyranosyl-oleanolate-3-yl-oxy)-succinyl-oxy] ethylpiperazin-1-yl} diazen-1-ium-1,2-diolate (8).** The title compound was obtained in 23% yield as a white powder; mp 140–143 °C; IR (KBr, cm⁻¹): 3423, 2946, 1735, 1641, 1462, 1161; ¹H NMR (DMSO-d₆, 300 MHz): δ 0.69 (s, 3H, CH₃), 0.80 (s, 6H, 2 × CH₃), 0.87–0.88 (m, 6H, 2 × CH₃), 1.10 (s, 3H, CH₃), 1.24 (s, 3H, CH₃), 2.55 (s, 4H, 2 × COCH₂), 2.72–2.78 (m, 1H, C₁₈-H), 3.12–3.14 (m, 4H, 2 × NCH₂), 3.32 (m, 4H, 2 × NCH₂), 3.45–3.47 (m, 2H,

2 × H₃), 3.60–3.65 (m, 2H, 2 × H₅), 4.02–4.04 (m, 1H, H₄), 4.11 (t, *J* = 5.4 Hz, 2H, NCH₂), 4.40–4.42 (m, 2H, OCH₂), 4.60 (t, *J* = 5.7 Hz, 1H, 3α-H), 4.88–4.91 (m, 1H, H₂), 4.98 (d, *J* = 4.8 Hz, 1H, H₂), 5.01–5.03 (m, 2H, C₁₂-H and H₆), 5.12 (d, *J* = 4.2 Hz, 1H, H₆), 5.16 (d, *J* = 5.4 Hz, 2H, 2 × H₆), 5.24 (d, *J* = 7.8 Hz, 1H, H₁), 5.41 (d, *J* = 4.8 Hz, 1H, H₁); ESI-MS: 1053 [M + H]⁺; HRMS: calculated for C₅₂H₈₅N₄O₁₈ [M + H]⁺: 1053.5853, found: 1053.5858, PPM error 0.47.

***O*²-β-D-Glucopyranosyl 1-{*N*-[(12-en-28-β-D-galactopyranosyl-oleanolate-3-yl-oxy)-succinyl-oxy]ethylpiperazin-1-yl} diazen-1-ium-1,2-diolate (9).** The title compound was obtained in 26% yield as a white powder; mp 142–145 °C; IR (KBr, cm⁻¹): 3420, 2946, 1735, 1631, 1463, 1161, 1147; ¹H NMR (DMSO-d₆, 300 MHz): δ 0.69 (s, 3H, CH₃), 0.80 (s, 6H, 2 × CH₃), 0.88 (s, 6H, 2 × CH₃), 1.10 (s, 3H, CH₃), 1.12–1.24 (m, 3H, CH₃), 2.55–2.60 (m, 4H, 2 × COCH₂), 2.73–3.79 (m, 1H, C₁₈-H), 3.17–3.21 (m, 4H, 2 × NCH₂), 3.40–3.43 (m, 4H, 2 × NCH₂), 3.45–3.51 (m, 2H, 2 × H₃), 3.63–3.72 (m, 3H, H₅ and NCH₂), 4.02–4.04 (m, 1H, H₅), 4.11 (t, *J* = 5.7 Hz, 2H, NCH₂), 4.38–4.47 (m, 1H, H₄), 4.50–4.51 (m, 1H, H₄), 4.55–4.62 (m, 2H, H₂ and 3α-H), 4.77 (d, *J* = 5.1 Hz, 1H, H₂), 4.90 (d, *J* = 7.8 Hz, 1H, H₆), 4.97 (d, *J* = 5.7 Hz, 1H, H₆), 5.03 (d, *J* = 5.1 Hz, 1H, H₆), 5.11–5.13 (m, 1H, H₆), 5.17 (brs, 1H, C₁₂-H), 5.21 (d, *J* = 7.5 Hz, 1H, H₁), 5.41 (d, *J* = 4.5 Hz, 1H, H₁); ESI-MS: 1053 [M + H]⁺; 1087 [M + Cl]⁻; HRMS: calculated for C₅₂H₈₅N₄O₁₈ [M + H]⁺: 1053.5853, found: 1053.5844, PPM error –0.85.

***O*²-β-D-Galactopyranosyl 1-{*N*-[(12-en-28-β-D-glucopyranosyl-oleanolate-3-yl-oxy)-succinyl-oxy]ethylpiperazin-1-yl} diazen-1-ium-1,2-diolate (10).** The title compound was obtained in 39% yield as a white powder; mp 144–146 °C. IR (KBr, cm⁻¹): 3421, 1734, 1645, 1464, 1231, 1160; ¹H NMR (CDCl₃, 300 MHz): δ 0.69 (s, 3H, CH₃), 0.80 (s, 6H, 2 × CH₃), 0.86–0.88 (m, 6H, 2 × CH₃), 1.09 (s, 3H, CH₃), 1.23 (s, 3H, CH₃), 2.55–2.58 (m, 4H, 2 × COCH₂), 3.08–3.17 (m, 4H, 2 × NCH₂), 3.41–3.54 (m, 4H, 2 × NCH₂), 3.61–3.66 (m, 2H, 2 × H₃), 4.09–4.11 (m, 2H, 2 × H₅), 4.37–4.44 (m, 2H, 2 × H₄), 4.54 (d, *J* = 4.5 Hz, 1H, H₂), 4.64–4.67 (m, 1H, 3α-H), 4.85 (d, *J* = 8.4 Hz, 1H, H₂), 4.90 (d, *J* = 5.7 Hz, 1H, H₆), 4.96 (d, *J* = 4.8 Hz, 1H, H₆), 5.02 (d, *J* = 4.8 Hz, 1H, H₆), 5.16–5.18 (m, 2H, H₁ and H₆), 5.22–5.26 (m, 1H, H₁); ESI-MS: 1053 [M + H]⁺; 1051 [M – H]⁻; HRMS: calculated for C₅₂H₈₅N₄O₁₈ [M + H]⁺: 1053.5853, found: 1053.5852, PPM error –0.09.

***O*²-β-D-Galactopyranosyl 1-{*N*-[(12-en-28-β-D-galactopyranosyl-oleanolate-3-yl-oxy)-succinyl-oxy]ethylpiperazine-1-yl} diazen-1-ium-1,2-diolate (11).** The title compound was obtained in 21% yield as a white powder; mp 141–143 °C; IR (KBr, cm⁻¹): 3421, 2923, 1735, 1643, 1464, 1231, 1147, 1069, 1003; ¹H NMR (CDCl₃, 300 MHz): δ 0.69 (s, 3H, CH₃), 0.80 (s, 2H, 2 × CH₃), 0.88 (s, 6H, 2 × CH₃), 1.10 (s, 3H, CH₃), 1.24 (s, 3H, CH₃), 2.55 (s, 4H, 2 × COCH₂), 3.49–3.53 (m, 2H, 2 × H₃), 3.66–3.67 (m, 2H, 2 × H₅), 4.11 (t, *J* = 4.8 Hz, 2H, OCH₂), 4.39–4.41 (m, 1H, H₄), 4.49–4.54 (m, 3H, 2 × H₂ and H₄), 4.62–4.67 (m, 1H, 3α-H), 4.75–4.78 (m, 1H, H₆), 4.84–4.90 (m, 2H, H₆ and H₆), 4.97 (d, *J* = 5.4 Hz, 1H, H₆), 5.16–5.25 (m, 3H, C₁₂-H and 2 × H₁); HRMS: calculated for C₅₂H₈₅N₄O₁₈ [M + H]⁺: 1053.5853, found: 1053.5852, PPM error –0.09.

***O*²-β-D-Glucopyranosyl 1-{*N*-[(12-en-28-β-D-glucopyranosyl-oleanolate-3-yl-oxy)-succinyl-oxy] ethyl-*N*-methylamino} diazen-1-ium-1,2-diolate (12).** The title compound was obtained in 19% yield as a white powder; mp 118–120 °C; IR (KBr, cm⁻¹): 3421, 2921, 1733, 1642, 1464, 1199, 1068, 1020; ¹H NMR (CDCl₃, 300 MHz): δ 0.69 (s, 3H, CH₃), 0.80 (s, 6H, 2 × CH₃), 0.89 (s, 6H, 2 × CH₃), 1.10 (s, 3H, CH₃), 1.24 (s, 3H, CH₃), 2.55 (s, 4H, 2 × COCH₂), 2.73–2.76 (m, 1H, C₁₈-H), 2.99 (s, 3H, NCH₃), 3.54–3.69 (m, 4H, 2 × H₃ and 2 × H₅), 4.15–4.18 (m, 2H, NCH₂), 4.35–4.48 (m, 3H, OCH₂ and H₄), 4.54–4.57 (m, 1H, 3α-H), 4.89 (d, *J* = 7.2 Hz, 1H, H₄), 4.95 (d, *J* = 4.8 Hz, 1H, H₂), 5.01–5.02 (m, 2H, H₂ and H₆), 5.11–5.13 (m, 1H, H₆), 5.15–5.17 (m, 2H, 2 × H₆), 5.24 (d, *J* = 8.1 Hz, 1H, H₁), 5.38 (d, *J* = 4.2 Hz, 1H, H₁); ESI-MS: 1016 [M + NH₄]⁺; 997 [M - H]⁻; HRMS: calculated for C₄₉H₇₉N₃O₁₈Na [M + Na]⁺:1020.5251, found: 1020.5252, PPM error 0.10.

***O*²-β-D-Glucopyranosyl 1-{*N*-[(12-en-28-β-D-galactopyranosyl-oleanolate-3-yl-oxy)-succinyl-oxy]ethyl-*N*-methylamino} diazen-1-ium-1,2-diolate (13).** The title compound was obtained in 20% yield as a white powder; mp 115–117 °C; IR (KBr, cm⁻¹): 3421, 2945, 1734, 1695, 1464, 1160, 1073; ¹H NMR (CDCl₃, 300 MHz): δ 0.69 (s, 3H, CH₃), 0.81 (s, 2H, 2 × CH₃), 0.86 (s, 6H, 2 × CH₃), 0.95 (s, 3H, CH₃), 1.11 (s, 3H, CH₃), 1.25 (s, 3H, CH₃), 2.72–2.79 (m, 1H, C₁₈-H), 2.99 (s, 3H, NCH₃), 3.62–3.68 (m, 2H, 2 × H₃), 4.14–4.19 (m, 2H, 2 × H₅), 4.38–4.40 (m, 1H, H₄), 4.50–4.58 (m, 3H, 2 × H₂ and H₄), 4.61–4.66 (m, 1H, 3α-H), 4.74–4.79 (m, 1H, H₆), 4.81–4.85 (m, 1H, H₆), 4.86–4.90 (m, 1H, H₆), 4.97–5.03 (m, 1H, H₆), 5.15–5.27 (m, 3H, C₁₂-H and 2 × H₁); ESI-MS: 1016 [M + NH₄]⁺; 1021 [M + Na]⁺; 997 [M - H]⁻; 1033 [M + Cl]⁻; HRMS: calculated for C₄₉H₇₉N₃O₁₈Na [M + Na]⁺:1020.5251, found: 1020.5203, PPM error -4.70.

***O*²-β-D-Galactopyranosyl 1-{*N*-[(12-en-28-β-D-glucopyranosyl-oleanolate-3-yl-oxy)-succinyl-oxy]ethyl-*N*-methylamino} diazen-1-ium-1,2-diolate (14).** The title compound was obtained in 20% yield as a white powder; mp 119–121 °C; IR (KBr, cm⁻¹): 3423, 2927, 1737, 1640, 1464, 1262, 1161, 1072; ¹H NMR (CDCl₃, 300 MHz): δ 0.68 (s, 3H, CH₃), 0.80 (s, 2H, 2 × CH₃), 0.88 (s, 6H, 2 × CH₃), 0.94 (s, 3H, CH₃), 1.09 (s, 3H, CH₃), 1.23 (s, 3H, CH₃), 2.72–2.76 (m, 1H, C₁₈-H), 2.97 (s, 3H, NCH₃), 3.66 (m, 2H, 2 × H₃), 4.14–4.16 (m, 2H, 2 × H₅), 4.38–4.41 (m, 1H, H₄), 4.51–4.54 (m, 3H, 2 × H₂ and H₄), 4.61–4.64 (m, 1H, 3α-H), 4.76–4.77 (m, 1H, H₆), 4.83–4.86 (m, 1H, H₆), 4.88–4.91 (m, 1H, H₆), 4.96–5.02 (m, 1H, H₆), 5.16–5.29 (m, 3H, C₁₂-H and 2 × H₁); ESI-MS: 1033 [M + Cl]⁻; HRMS: calculated for C₄₉H₇₉N₃O₁₈Na [M + Na]⁺:1020.5251, found: 1020.5242, PPM error -0.88.

***O*²-β-D-Galactopyranosyl 1-{*N*-[(12-en-28-β-D-galactopyranosyl-oleanolate-3-yl-oxy)-succinyl-oxy]ethyl-*N*-methylamino} diazen-1-ium-1,2-diolate (15).** The title compound was obtained in 34% yield as a white powder; mp 115–117 °C; IR (KBr, cm⁻¹): 3449, 3328, 1734, 1627, 1576, 1438, 1369, 1312; ¹H NMR (CDCl₃, 300 MHz): δ 0.68 (s, 3H, CH₃), 0.80 (s, 2H, 2 × CH₃), 0.88 (s, 6H, 2 × CH₃), 0.94 (s, 3H, CH₃), 1.09 (s, 3H, CH₃), 1.23 (s, 3H, CH₃), 2.72–2.76 (m, 1H, C₁₈-H), 2.97 (s, 3H, NCH₃), 3.65–3.69 (m, 2H, 2 × H₃), 4.14–4.16 (m, 2H, 2 × H₅), 4.38–4.41 (m, 1H, H₄), 4.51–4.54 (m, 3H, 2 × H₂ and H₄),

4.60–4.65 (m, 1H, 3α-H), 4.76–4.77 (m, 1H, H₆), 4.83–4.86 (m, 1H, H₆), 4.88–4.92 (m, 1H, H₆), 4.98 (d, *J* = 5.4 Hz, 1H, H₆), 5.16 (brs, 1H, C₁₂-H), 5.20–5.24 (m, 2H, 2 × H₁); ESI-MS: 1016 [M + NH₄]⁺; 1021 [M + Na]⁺; HRMS: calculated for C₄₉H₇₉N₃O₁₈Na [M + Na]⁺:1020.5251, found: 1020.5243, PPM error -0.78.

***O*²-β-D-Glucopyranosyl 1-{*N*-[(12-en-28-β-D-glucopyranosyl-oleanolate-3-yl-oxy)-succinyl] piperazin-1-yl} diazen-1-ium-1,2-diolate (16).** The title compound was obtained in 45% yield as a white powder; mp 181–183 °C; IR (KBr, cm⁻¹): 3423, 2945, 1729, 1640, 1466, 1387, 1231, 1177; ¹H NMR (CDCl₃, 300 MHz): δ 0.69 (s, 3H, CH₃), 0.80 (s, 6H, 2 × CH₃), 0.87–0.88 (m, 6H, 2 × CH₃), 1.10 (s, 3H, CH₃), 1.18–1.24 (m, 3H, CH₃), 2.73–2.75 (m, 1H, C₁₈-H), 3.56–3.65 (m, 4H, 2 × H₅ and 2 × H₃), 4.33–4.44 (m, 1H, H₄), 4.40–4.44 (m, 2H, 2 × H₄), 4.54 (d, *J* = 4.8 Hz, 1H, H₂), 4.76 (d, *J* = 5.4 Hz, 1H, H₂), 4.62–4.67 (m, 1H, 3α-H), 4.86–4.92 (m, 2H, H₂ and H₆), 4.94 (d, *J* = 4.5 Hz, 1H, H₆), 5.01 (d, *J* = 4.5 Hz, 1H, H₆), 5.16–5.18 (m, 2H, H₆ and C₁₂-H), 5.22–5.27 (m, 2H, 2 × H₁); ESI-MS: 1043 [M + Cl]⁻; HRMS: calculated for C₅₀H₈₀N₄O₁₇Na [M + Na]⁺:1031.5411, found: 1031.5412, PPM error 0.10.

***O*²-β-D-Glucopyranosyl 1-{*N*-[(12-en-28-β-D-galactopyranosyl-oleanolate-3-yl-oxy)-succinyl] piperazin-1-yl} diazen-1-ium-1,2-diolate (17).** The title compound was obtained in 40% yield as a white powder; mp 182–184 °C; IR (KBr, cm⁻¹): 3431, 1730, 1640, 1466, 1231, 1177, 1146; ¹H NMR (CDCl₃, 300 MHz): δ 0.69 (s, 3H, CH₃), 0.80 (s, 6H, 2 × CH₃), 0.88 (s, 9H, 3 × CH₃), 1.10 (s, 3H, CH₃), 2.60–2.61 (m, 4H, 2 × COCH₂), 2.75–2.81 (m, 1H, C₁₈-H), 3.22–3.26 (m, 4H, 2 × NCH₂), 3.30–3.40 (m, 4H, 2 × NCH₂), 3.45–3.47 (m, 2H, 2 × H₃), 3.60–3.63 (m, 2H, 2 × H₅), 4.35–4.42 (m, 1H, H₄), 4.50 (d, *J* = 4.2 Hz, 1H, H₄), 4.55–4.60 (m, 2H, 3α-H and H₂), 4.77 (d, *J* = 5.4 Hz, 1H, H₂), 4.90–4.93 (m, 1H, H₆), 4.98 (d, *J* = 6.0 Hz, 1H, H₆), 5.03 (d, *J* = 5.4 Hz, 1H, H₆), 5.13–5.16 (m, 2H, H₆ and C₁₂-H), 5.21 (d, *J* = 7.8 Hz, 1H, H₁), 5.42 (d, *J* = 4.8 Hz, 1H, H₁); ESI-MS: 1043 [M + Cl]⁻; HRMS: calculated for C₅₀H₈₀N₄O₁₇Na [M + Na]⁺:1031.5411, found: 1031.5417, PPM error 0.58.

***O*²-β-D-Galactopyranosyl 1-{*N*-[(12-en-28-β-D-glucopyranosyl-oleanolate-3-yl-oxy)-succinyl] piperazin-1-yl} diazen-1-ium-1,2-diolate (18).** The title compound was obtained in 52% yield as a white powder; mp 184–186 °C; IR (KBr, cm⁻¹): 3423, 2921, 2851, 1731, 1640, 1465, 1231; ¹H NMR (CDCl₃, 300 MHz): δ 0.69 (s, 3H, CH₃), 0.80 (s, 2H, 2 × CH₃), 0.86–0.88 (m, 6H, 2 × CH₃), 1.09 (s, 3H, CH₃), 1.23 (s, 3H, CH₃), 2.72–2.75 (m, 1H, C₁₈-H), 3.61–3.64 (m, 4H, 2 × H₃ and 2 × H₅), 4.37–4.44 (m, 1H, 2 × H₄), 4.54 (d, *J* = 4.2 Hz, 1H, H₂), 4.65 (m, 1H, 3α-H), 4.85–4.92 (m, 2H, C₁₂-H and H₆), 5.01 (d, *J* = 4.5 Hz, 1H, H₆), 5.16–5.18 (m, 2H, 2 × H₆), 5.22–5.27 (m, 2H, 2 × H₁); ESI-MS: 1026 [M + NH₄]⁺; 1043 [M + Cl]⁻; HRMS: calculated for C₅₀H₈₀N₄O₁₇Na [M + Na]⁺:1031.5411, found: 1031.5416, PPM error 0.48.

***O*²-β-D-Galactopyranosyl 1-{*N*-[(12-en-28-β-D-galactopyranosyl-oleanolate-3-yl-oxy)-succinyl] piperazin-1-yl} diazen-1-ium-1,2-diolate (19).** The title compound was obtained in 39% yield as a white powder; mp 185–188 °C; IR (KBr, cm⁻¹): 3431,

2945, 1731, 1640, 1466, 1231; ^1H NMR (CDCl_3 , 300 MHz): δ 0.69 (s, 3H, CH_3), 0.80 (s, 6H, $2 \times \text{CH}_3$), 0.88 (s, 9H, $3 \times \text{CH}_3$), 1.10 (s, 3H, CH_3), 1.24 (s, 3H, CH_3), 2.73–2.77 (m, 1H, $\text{C}_{18}\text{-H}$), 3.40–3.47 (m, 4H, $2 \times \text{NCH}_2$), 3.49–3.55 (m, 4H, $2 \times \text{NCH}_2$), 3.61–3.68 (m, 4H, $2 \times \text{H}_3$ and $2 \times \text{H}_5$), 4.36–4.41 (m, 1H, H_4), 4.51 (d, $J = 4.5$ Hz, 1H, H_4), 4.54–4.58 (m, 2H, $2 \times \text{H}_2$), 4.63–4.68 (m, 1H, $3\alpha\text{-H}$), 4.77 (d, $J = 5.1$ Hz, 1H, H_6'), 4.86–4.89 (m, 1H, H_6'), 4.90–4.92 (m, 1H, H_6), 4.98 (d, $J = 5.4$ Hz, 1H, H_6), 5.16 (brs, 1H, $\text{C}_{12}\text{-H}$), 5.21 (d, $J = 7.5$ Hz, 1H, H_1), 5.27 (d, $J = 5.7$ Hz, 1H, H_1); ESI-MS: 1007 $[\text{M} - \text{H}]^-$; 1043 $[\text{M} + \text{Cl}]^-$; HRMS: calculated for $\text{C}_{50}\text{H}_{80}\text{N}_4\text{O}_{17}\text{Na}$ $[\text{M} + \text{Na}]^+$: 1031.5411, found: 1031.5404, PPM error -0.68 .

MTT assay

Human HCC SMMC-7721, HepG2 or non-tumor liver LO2 cells at 10^4 cells per well were cultured in 10% FBS DMEM in 96-well flat-bottom microplates overnight. The cells were incubated in triplicate with, or without, different concentrations of each test compound for various periods. During the last 4 h incubation, 30 μL of tetrazolium dye (MTT) solution (5 mg mL^{-1}) was added to each well. The resulting MTT-formazan crystals were dissolved in 150 μL DMSO, and absorbance was measured spectrophotometrically at 570 nm using an ELISA plate reader. The inhibition induced by each test compound at the indicated concentrations was expressed as a percentage ($(1 - \text{the optical density ratio of the treatment to vehicle control}) \times 100\%$). Additional experiments were performed by pre-treatment of HepG2 cells with, or without, 20 mM hemoglobin for 1 h and exposure to individual compounds tested.

Nitrate–nitrite measurement *in vitro*

The levels of NO were determined using a nitrate–nitrite colorimetric assay kit (Beyotime Institute of Biotechnology), according to the manufacturers' instructions. The cells (5×10^6 per well) were treated in triplicate with different concentrations of the test compound for 6 h and lysed. After microfuge ultrafiltration, the contents of nitrate–nitrite in the lysates were measured. Individual values were obtained by subtracting the background (vehicle treated wells) and the amount of nitrite–nitrate was calculated, according to the standard curve.

Acute toxicity

Seven-week-old male and female KM mice, purchased from the Shanghai Laboratory Animal Center (Shanghai, China), were housed in a pathogen free facility. Groups of mice ($n = 10$ per group) were injected intravenously with a single dose of 200, 180, 162, 145.8 mg kg^{-1} or vehicle control, respectively. Mouse survival was monitored up to 14 days after treatment. The experimental protocols were evaluated and approved by the Ethics Committee of China Pharmaceutical University.

In vivo tumor growth inhibition

Female BALB/c nude mice 5–6 weeks of age, purchased from the Institute of Laboratory Animal Science, Chinese Academy of

Medical Sciences, were inoculated subcutaneously with 10^6 SMMC-7721 cells. After the formation of a solid tumor with a volume of about 100–300 mm^3 , the tumor-bearing mice were randomized and treated intravenously with 3 mg kg^{-1} of **6**, or vehicle alone (0.4 mL) three times per week for 21 days, respectively. The growth of implanted tumors in mice and their body weights were measured every three days, as described previously.⁶ At the end of the experiment, the mice were sacrificed, their tumors were dissected, and the tumor size and weight were measured.

Flow cytometry assay of cell apoptosis

SMMC-7721 cells were cultured overnight and incubated in triplicate with the test compound (1.5, 3.0 and 6.0 μM) or vehicle for 48 h. The cells were harvested, and stained with FITC-Annexin V and PI at room temperature for 15 min. The percentage of apoptotic cells were determined by flow cytometry analysis.

Cell mitochondrial membrane potential assay

SMMC-7721 cells were cultured overnight and incubated in triplicate with the test compound (1.5, 3.0 and 6.0 μM) or vehicle for 48 h. The cells were stained with JC-1 dye, according to the manufacturer's instruction (Keygen, KGA601). The percentage of cells with healthy or collapsed mitochondrial membrane potentials was monitored by flow cytometry analysis ($\text{Ex} = 488 \text{ nm}$; $\text{Em} = 530 \text{ nm}$).

Western blotting assays

SMCC-7721 cells were incubated in triplicate with different doses of **6** for 48 h, the cells were harvested, the cells were lysed using lysis buffer, and solution was centrifuged. After the protein concentrations were determined, individual cell lysates (50 μg per lane) were separated by sodium dodecyl sulfate polyacrylamide gel electrophoresis (10% gel, SDS-PAGE) and transferred onto nitrocellulose membranes. After being blocked with 5% fat-free milk, the target proteins in the membranes were probed with monoclonal anti-Bax (KGA714), anti-Bcl2 (KGA715), anti-caspase 3 (KGA717), anti-caspase 9 (KGA720), anti-cyto C (KGA723) and anti- β -actin antibodies (KGA731, KeyGEN Biotech, Nanjing, China), respectively. The bound antibodies were detected by horse radish peroxidase (HRP)-conjugated second antibodies and visualized using the enhanced chemiluminescent reagent. The relative levels of each signaling event to control β -actin were determined by densitometric scanning.

Assay of caspase 3, and 9 activity

The activities of caspase 3 and 9 were determined by enzymatic assays using caspase 3 and 9 colorimetric assay kits, according to the manufacturers' instructions (Keygen, KGA202, KGA402). Briefly, SMCC-7721 cells ($3\text{--}5 \times 10^6$ per well) were incubated in duplicate with compound **6** (at 0, 1.5, 3.0 and 6.0 μM) for 48 h. The cells were harvested and lysed in 50 μL of lysis buffer

(with 0.5 μ L DTT) prior to centrifugation. After determining the concentrations of proteins in the supernatants, the cell lysates were reacted with 5 μ L caspase 3 or 9 substrates at 37 $^{\circ}$ C for 4 h, and the enzymatic activities were measured at 405 nm using a microplate reader. The relative levels of enzymatic activities in individual samples compared to the untreated controls were calculated.

Notes and references

- 1 L. R. Roberts and G. J. Gores, *Expert Opin. Emerging Drugs*, 2006, **11**, 469–487.
- 2 D. A. Wink, Y. Vodovotz, J. A. Cook, M. C. Krishna, S. Kim, D. Coffin, W. DeGraff, A. M. Deluca, J. Liebmann and J. B. Mitchell, *Biochemistry (Moscow)*, 1998, **63**, 802–809.
- 3 L. J. Hofseth, S. P. Hussain, G. N. Wogan and C. C. Harris, *Free Radical Biol. Med.*, 2003, **34**, 955–968.
- 4 D. W. Jeong, Y. H. Kim, H. H. Kim, H. Y. Ji, S. D. Yoo, W. R. Choi, S. M. Lee, C. K. Han and H. S. Lee, *Biopharm. Drug Dispos.*, 2007, **28**, 51–57.
- 5 L. Cipak, L. Grausova, E. Miadokova, L. Novotny and P. Rauko, *Arch. Toxicol.*, 2006, **80**, 429–435.
- 6 L. Chen, Y. Zhang, X. Kong, E. Lan, Z. Huang, S. Peng, D. L. Kaufman and J. Tian, *J. Med. Chem.*, 2008, **51**, 4834–4838.
- 7 Z. Huang, Y. Zhang, L. Zhao, Y. Jing, Y. Lai, L. Zhang, Q. Guo, S. Yuan, J. Zhang, L. Chen, S. Peng and J. Tian, *Org. Biomol. Chem.*, 2010, **8**, 632–639.
- 8 C. M. Maragos, D. Morley, D. A. Wink, T. M. Dunams, J. E. Saavedra, A. Hoffman, A. A. Bove, L. Isaac, J. A. Hrabie and L. K. Keefer, *J. Med. Chem.*, 1991, **34**, 3242–3247.
- 9 P. J. Shami, J. E. Saavedra, C. L. Bonifant, J. Chu, V. Udupi, S. Malaviya, B. I. Carr, S. Kar, M. Wang, L. Jia, X. Ji and L. K. Keefer, *J. Med. Chem.*, 2006, **49**, 4356–4366.
- 10 J. E. Saavedra, A. Srinivasan, G. S. Buzard, K. M. Davies, D. J. Waterhouse, K. Inami, T. C. Wilde, M. L. Citro, M. Cuellar, J. R. Deschamps, D. Parrish, P. J. Shami, V. J. Findlay, D. M. Townsend, K. D. Tew, S. Singh, L. Jia, X. Ji and L. K. Keefer, *J. Med. Chem.*, 2006, **49**, 1157–1164.
- 11 X. Wu, X. Tang, M. Xian and P. G. Wang, *Tetrahedron Lett.*, 2001, **42**, 3779–3782.
- 12 C. Chen, Y. Shi, S. Li, Q. Qi, L. Gu, J. Song and P. G. Wang, *Arch. Pharm.*, 2006, **339**, 366–371.
- 13 Y. Hou, X. Wu, W. Xie, P. G. Braunschweiger and P. G. Wang, *Tetrahedron Lett.*, 2001, **42**, 825–829.
- 14 X. Wu, X. Tang, M. Xian, P. G. Braunschweiger and P. G. Wang, *Bioorg. Med. Chem.*, 2002, **10**, 2303–2307.
- 15 Z. Huang, Y. Zhang, L. Fang, Z. Zhang, Y. Lai, Y. Ding, F. Cao, J. Zhang and S. Peng, *Chem. Commun.*, 2009, 1763–1765.
- 16 C. S. Cheung, K. K. Chung, J. C. Lui, C. P. Lau, P. M. Hon, J. Y. Chan, K. P. Fung and S. W. Au, *Cancer Lett.*, 2007, **253**, 224–235.
- 17 P. Gong, A. I. Cederbaum and N. Nieto, *Mol. Pharmacol.*, 2004, **65**, 130–138.
- 18 D. Fukumura, S. Kashiwagi and R. K. Jain, *Nat. Rev. Cancer*, 2006, **6**, 521–534.
- 19 D. A. Langer, A. Das, D. Semela, N. Kang-Decker, H. Hendrickson, S. F. Bronk, Z. S. Katusic, G. J. Gores and V. H. Shah, *Hepatology*, 2008, **47**, 1983–1993.
- 20 K. M. Boatright and G. S. Salvesen, *Curr. Opin. Cell Biol.*, 2003, **15**, 725–731.
- 21 M. O. Hengartner, *Nature*, 2000, **407**, 770–776.
- 22 X. Wang, *Genes Dev.*, 2001, **15**, 2922–2933.
- 23 L. P. Billen, C. L. Kokoski, J. F. Lovell, B. Leber and D. W. Andrews, *PLoS Biol.*, 2008, **6**, e147.
- 24 I. Marzo and J. Naval, *Biochem. Pharmacol.*, 2008, **76**, 939–946.